

# **Appendix to “A Unified Model of Cohort Mortality”**

**by Adriana Lleras-Muney and Flavien Moreau**

## **Contents**

**Appendix A:** Figures and Tables

**Appendix B:** Review of existing models of mortality and contribution

**Appendix C:** Mathematical appendix

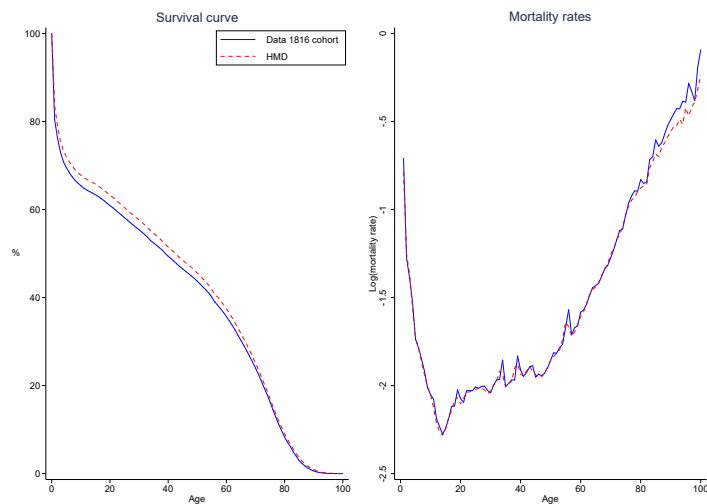
**Appendix D:** Notes on the empirical methods

**Appendix E:** Implications for optimal investments

**References**

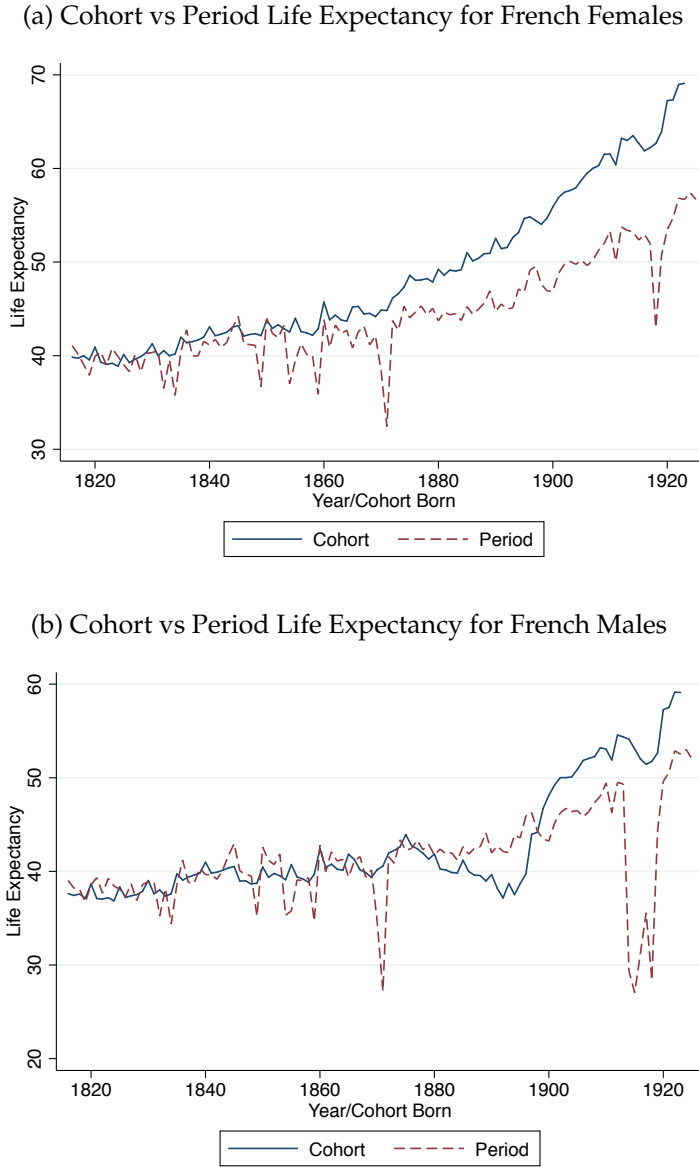
## Appendix A: Figures & Tables

Figure A9: Comparison of  $q$ -rate in the paper and in the HMD (1816)



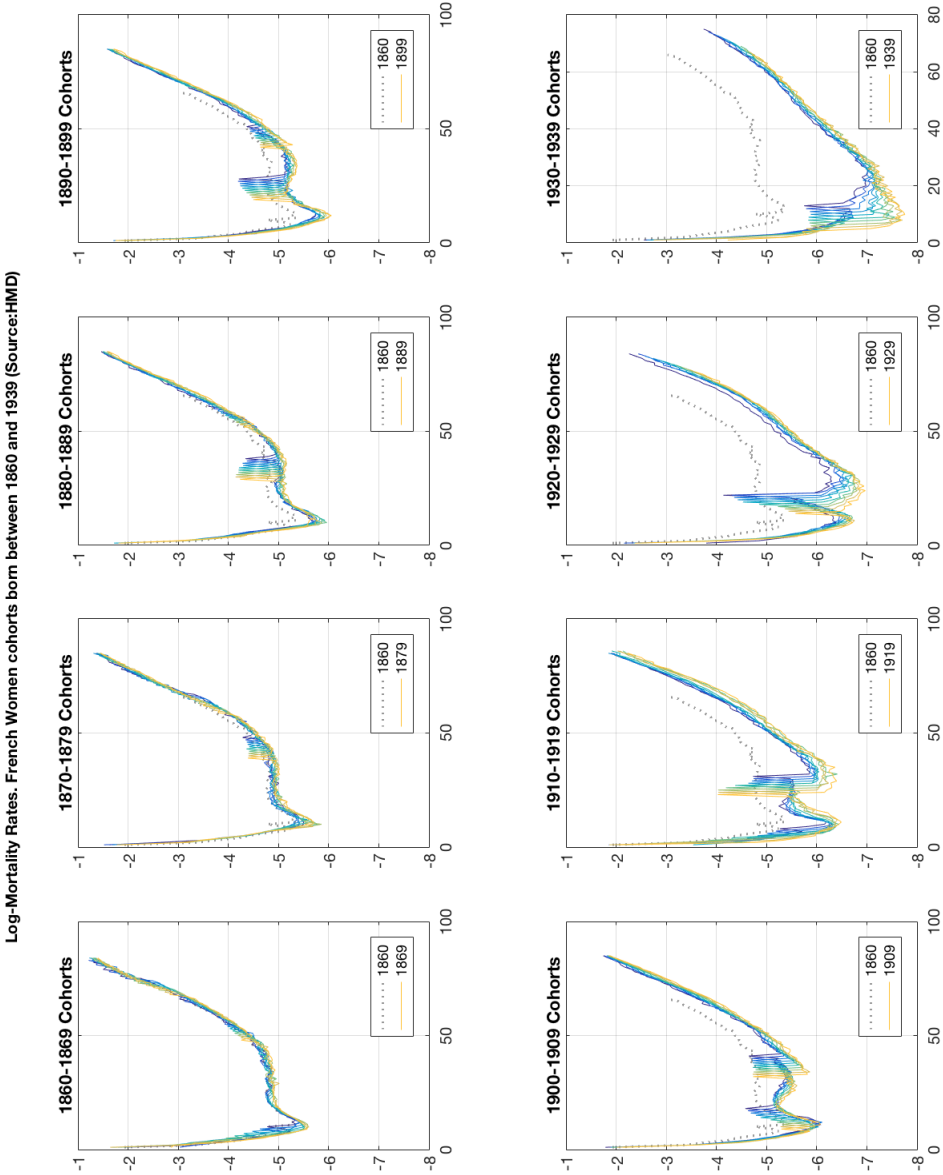
Note: The life expectancy is 38.25 years with the  $q$  we use (see Appendix D), to be compared with 39.86 with the  $q$  in HMD and 39.83 years for the life expectancy computed by the HMD itself following a more involved statistical methodology.

Figure A10: Cohort vs. Period statistics, French Women 1860 and 1940



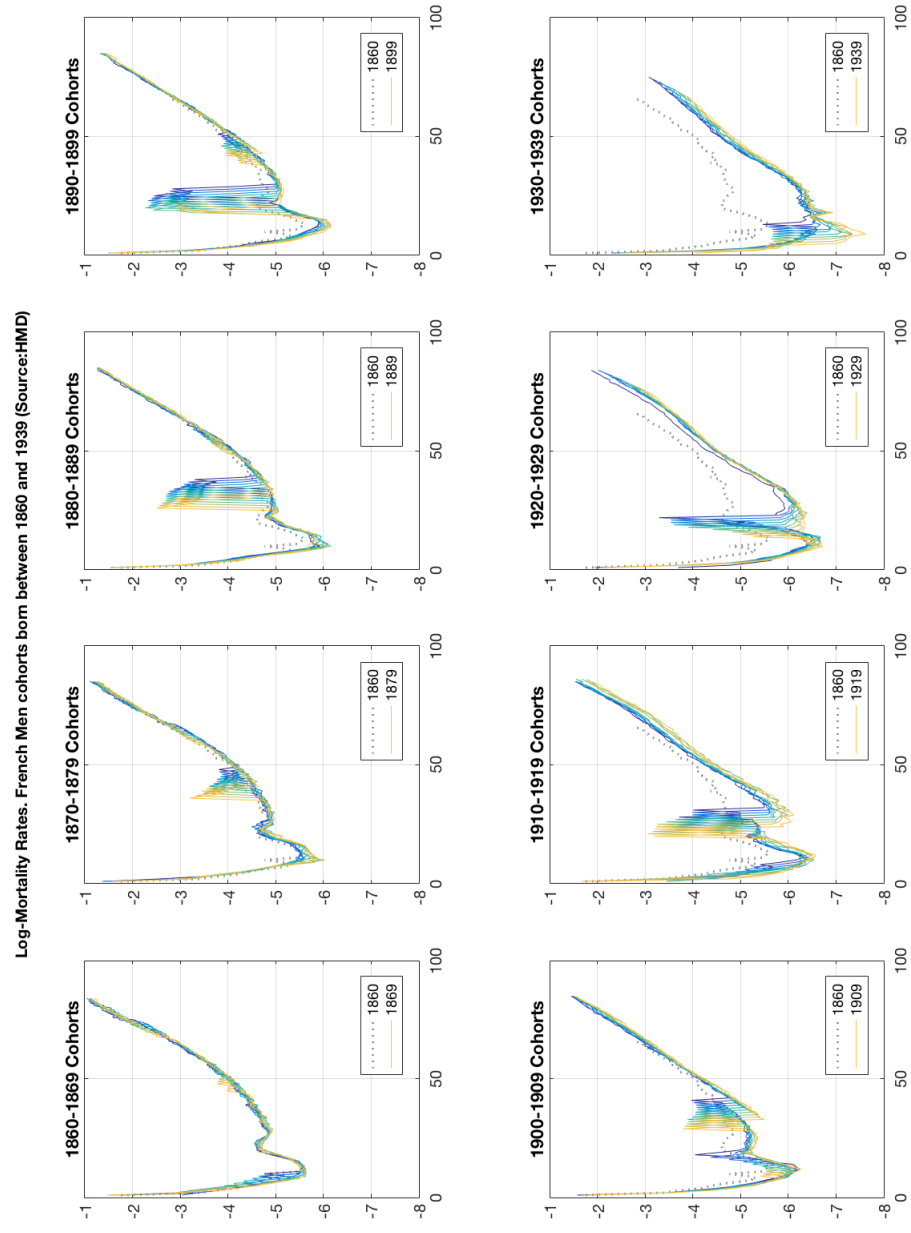
Note: Data from the Human Mortality Database. *Panel a* shows that period and cohort life expectancy for French females were almost identical for the cohort borns before 1860, suggesting that for these cohorts the assumption of stationarity holds, but starting sometime in the late 19th century the curves diverge and cohort life expectancy exceeds period life expectancy substantially. This occurs because the period life expectancy overestimates the mortality rates that the cohort will experience at older ages due to improvements in mortality. *Panel b* shows the period and cohort life expectancy of French men since 1816. The two series are almost the same up to roughly 1880 and they diverge after, with the cohort life expectancy exceeding the period life expectancy substantially by the end of the period. For men the cohort life expectancy does not rise monotonically. We observe that actual (cohort) life expectancy is lower than predicted (period) life expectancy for cohorts born between 1880 and 1900, likely as a result of WWI and WWII.

Figure A11: Age profile of mortality of women born in France between 1860 and 1940, by decade



Note: Human Mortality Data

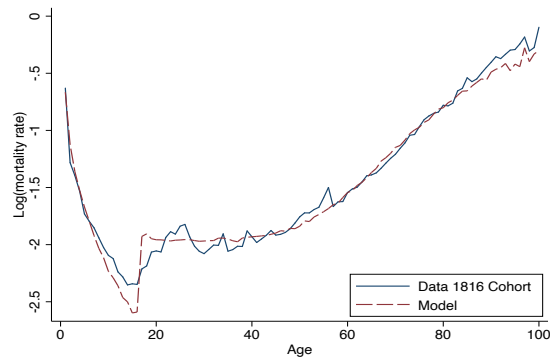
Figure A12: Age profile of mortality of men born in France between 1860 and 1940, by decade



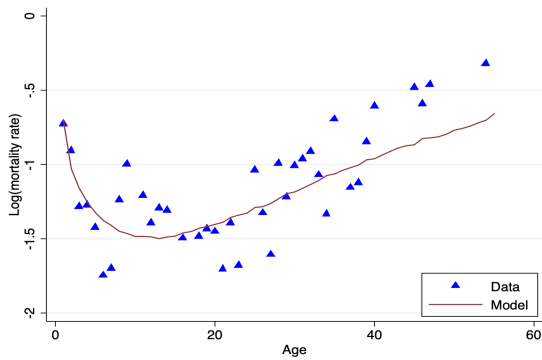
Note: Human Mortality Data

Figure A13: Model fit for humans and primates

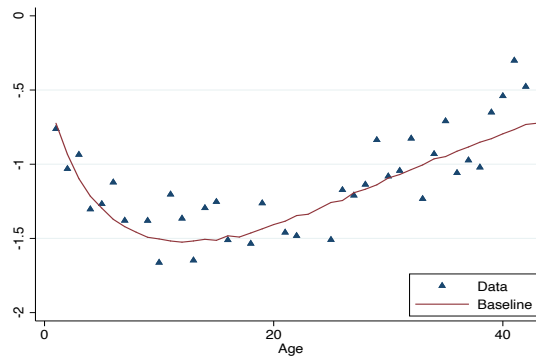
(a) French men born in 1816



(b) Female chimpanzees

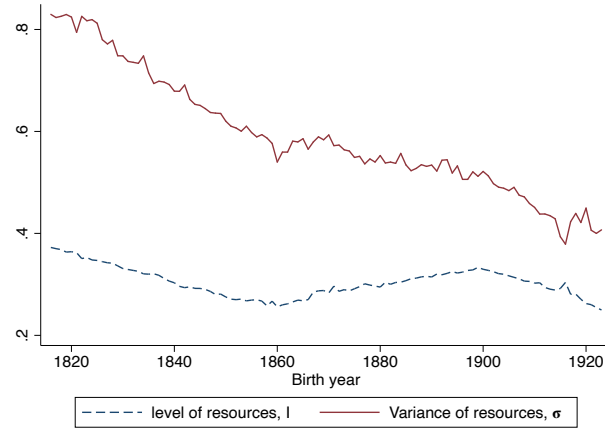


(c) Male chimpanzees



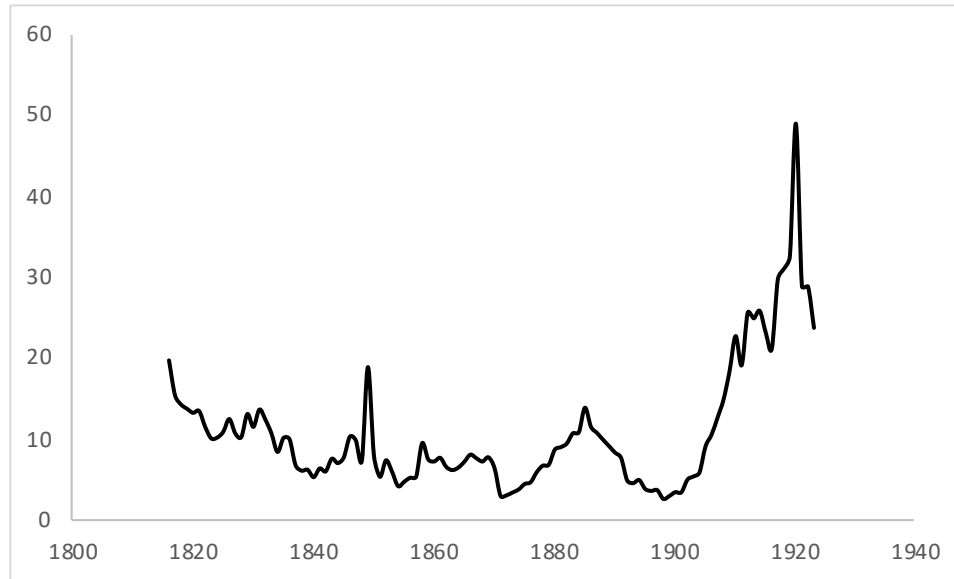
Note: *Panel a* shows the observed and predicted mortality rates for French men born in 1816. Appendix Table 1 show the estimated parameters for men. *Panel b* shows the data and estimated mortality rates for female chimps. *Panel c* shows the data and estimated mortality for male chimps. Appendix Table 3 show the estimated parameters for chimps.

Figure A14: Health Resources and Variance of Health Resources



Note: Figure shows the estimates for  $I$  and  $\sigma$ , the level of health resources and its variance for all cohorts.

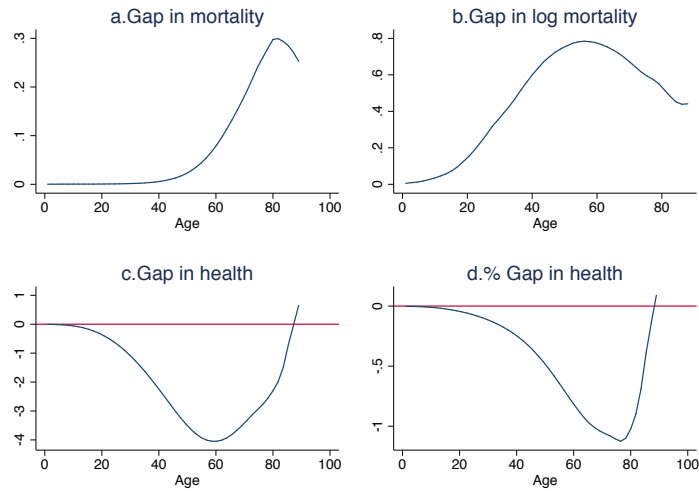
Figure A15: Model fit for birth cohorts born 1816-1923



Note: this figure shows the fit of the model for each birth cohort. The fit is measured as the sum of quadratic errors between the estimated survival curve and the data at each age, defined as  $\sum_a (\hat{S}_a - S_a)^2$ . A lower number indicates a greater fit (smaller errors).



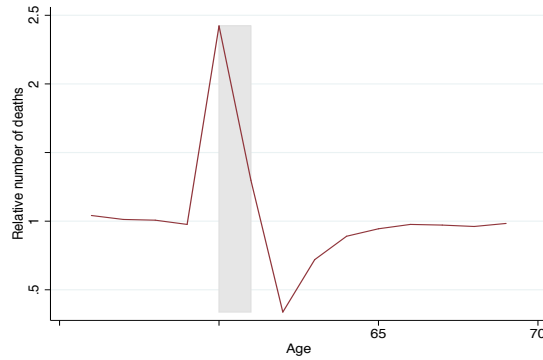
Figure A16: Increasing the lifetime depreciation rate by 50% by age



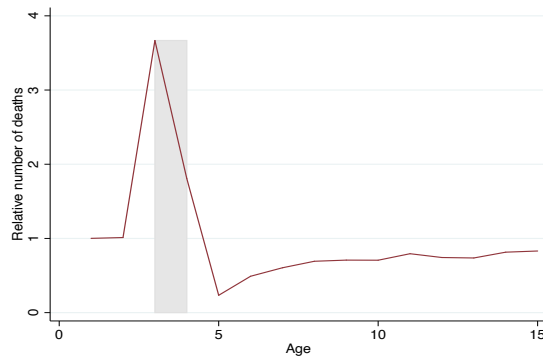
Note: The Figure shows the gap in mortality or health between a baseline population and a population with a 50% higher depreciation rate  $\delta$ . Gap is computed as  $MR(\text{low}) - MR(\text{high})$ , or  $H(\text{low}) - H(\text{high})$ . The figures become very noisy after age 90 because there are almost no survivors, so we do not include these data points. Simulated data for two population of 500,000 individuals each. The baseline parameters are the same as in Figure 3.

Figure A17: The effects of temporary increases in the threshold

(a) Harvesting in the model among the old

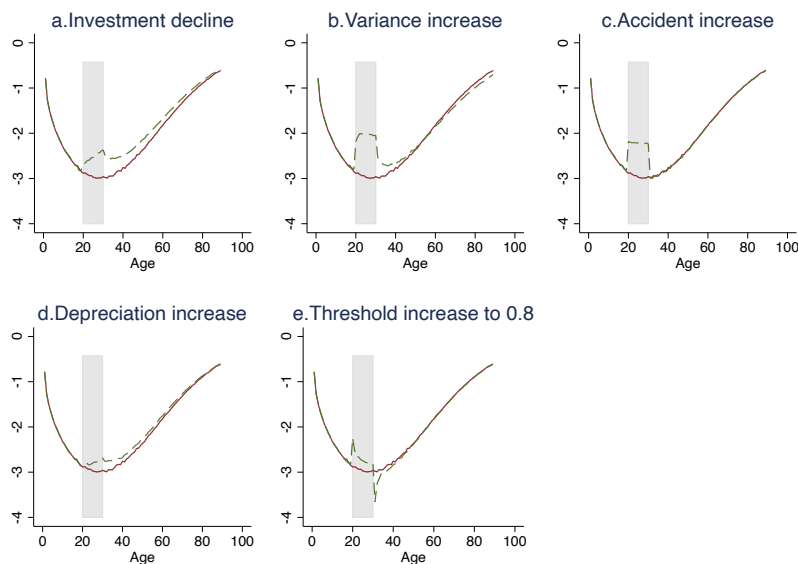


(b) Harvesting in the model among the young



Note: We follow Toulemon and Barbieri (2008) and show the mortality displacement created by the French 2003 Heatwave. The number of excess deaths in Summer 2003 is computed relative to the number of deaths during the same period in 2000. The grey (hatched) area corresponds to an excess (deficit) of 15,000 deaths. These excess deaths are computed for the entire population. *Panel a* shows the simulated effects of a temporary increase in the threshold (from 0 to 0.8) at ages 60 and 61 on the 1816 French cohort (setting the accident rate to 0 for simplicity and using the parameters from Figure 3) which results in approximately 8,000 excess deaths during the shock and fewer deaths for the subsequent 2 years. *Panel b* shows the simulated effects of a temporary increase in the threshold (from 0 to 0.8) at ages 3 and 4 on the 1816 French cohort (setting the accident rate to 0 for simplicity) which results in approximately 40,000 excess deaths during the shock. The effect is much larger among the young because many more children are close to the threshold as shown in Figure 3a. But the displacement effect is spread out over a much longer period for children.

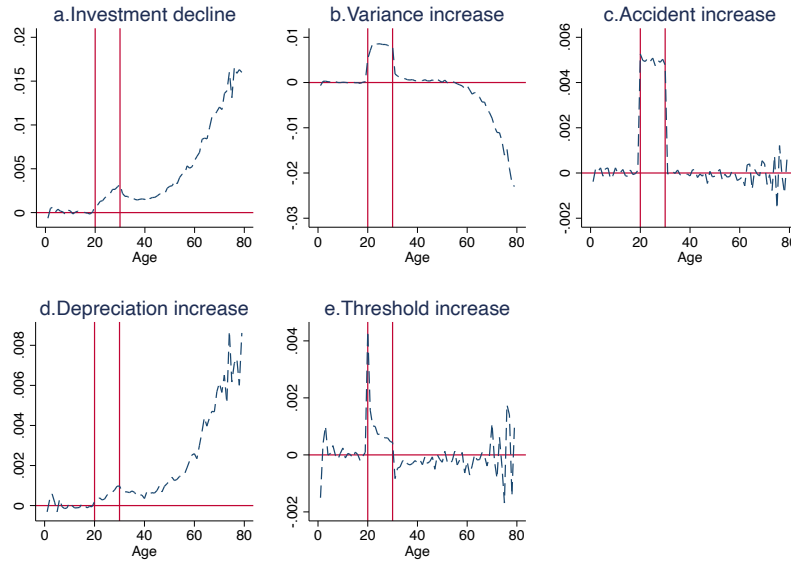
Figure A18: Effects of temporary shocks on log mortality rates



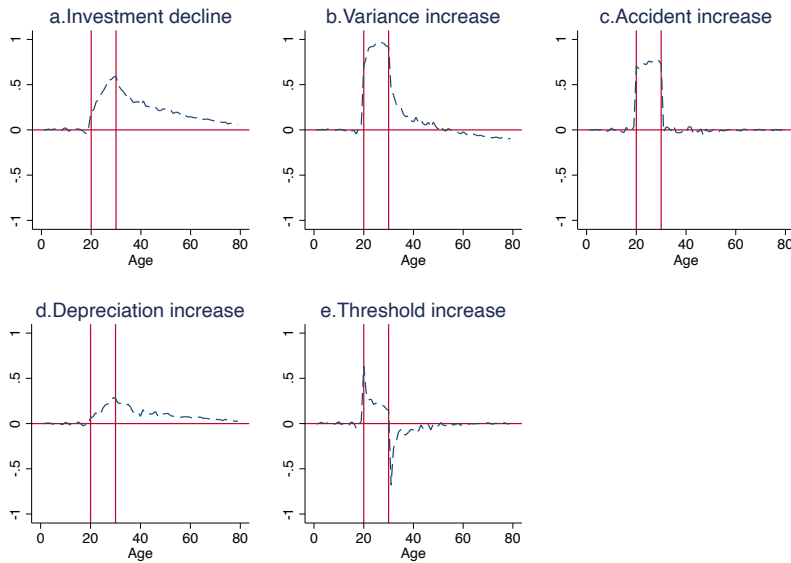
Note: Results from simulations using the 1816 cohort parameters and assuming no adolescent hump. Shocks correspond to a 50% change in the parameter, except for the threshold, which is assumed to increase to 0.8 from 0. The shock starts at age 20 and lasts 10 years, ending at age 30.

Figure A19: Effect of exogenous temporary shocks at age 20

(a) Gaps in mortality



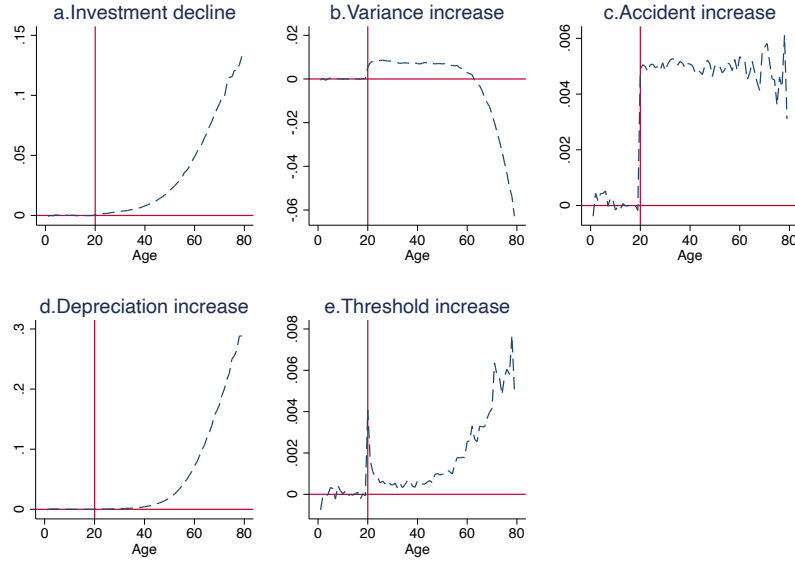
(b) Gaps in log mortality



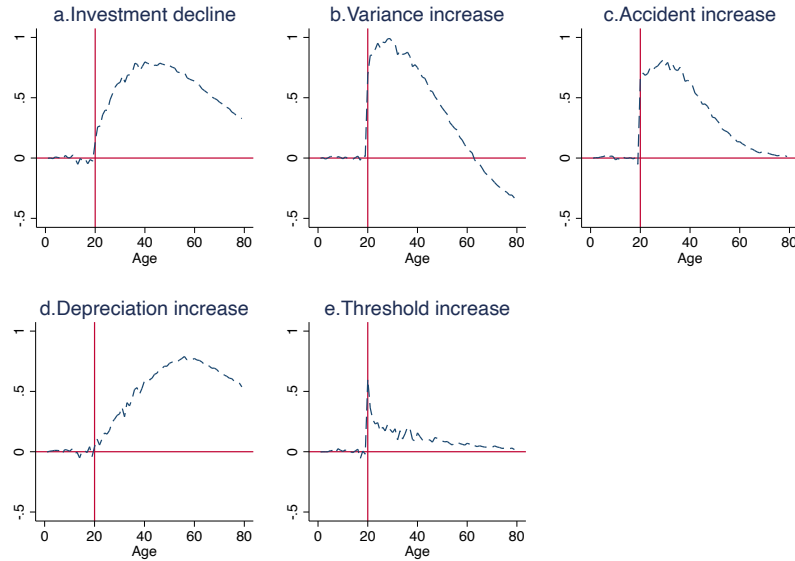
Note: The figure shows the effects of a temporary change in a single parameter occurring at age 20 in a simple model without adolescent humps. The shock lasts for 10 years, ending at age 30. Each figure shows the different in mortality that results from a temporary shock, relative to the counterfactual of no shock. In essence these figures plot the pattern that would be predicted in an event study, where the coefficient of a dummy for the affected population is interacted with time fixed effects. *Panel a* shows the gaps in levels and *panel b* shows the gaps in logs. The gaps in levels are not shown in the same scale to make the patterns more apparent. The baseline parameters are the same as in Figure 3.

Figure A20: Effects of exogenous permanent shocks at age 20

(a) Gaps in mortality

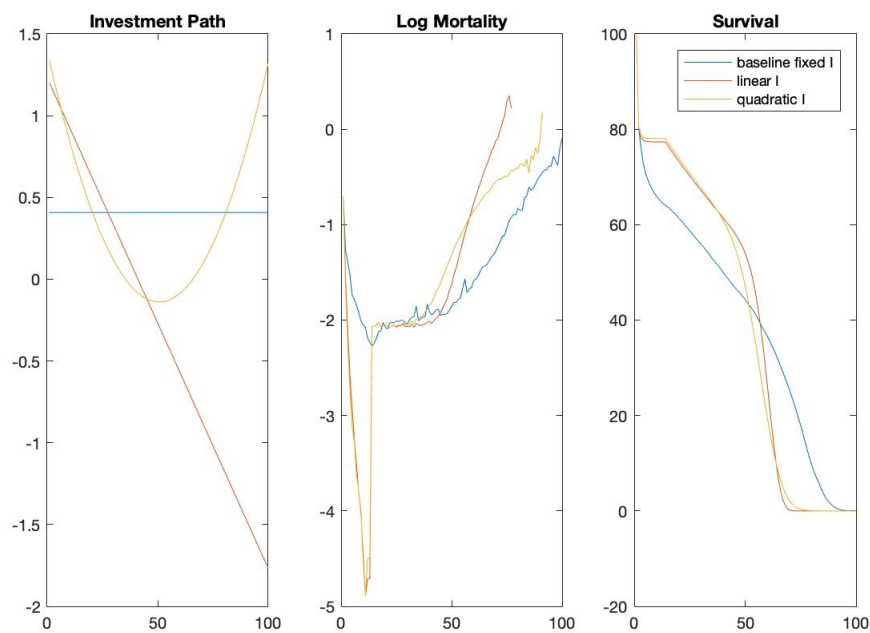


(b) Gaps in log mortality



Note: The figure shows the effects of a permanent change in a single parameter occurring at age 20 in a simple model without adolescent humps. Each figure shows the different in mortality that results from a temporary shock, relative to the counterfactual of no shock. In essence these figures plot the pattern that would be predicted in an event study, where the coefficient of a dummy for the affected population is interacted with time fixed effects. *Panel a* shows the gaps in levels and *panel b* shows the gaps in logs. The gaps in levels are not shown in the same scale to make the patterns more apparent. The baseline parameters are the same as in Figure 3.

Figure A21: Optimal Investment Levels by Age



Note: The first panel represents the estimated investment path when investment is constrained to be constant (blue line), linear (red line), or quadratic (yellow). In the second and third panel, 1816 cohort data is represented in blue. Both linear and quadratic optimal investment paths would devote more resources to younger cohorts, reducing mortality rates in the early years.

Table A1: Modeling prime-age mortality. French Cohort born in 1816

Gender	(1)		(2)		(3)		(4)	
	Females				Males			
Model		Baseline	With adolescent hump		Baseline	With adolescent hump		
Initial mean health	$\mu_H$	0.9115	0.8634		0.7091	0.7104		
Investment	$I$	0.1336	0.4075		0.1209	0.4432		
Standard Deviation of Shock	$\sigma_e$	0.5556	1.0241		0.4700	1.0785		
Depreciation	$\delta$	0.0010	0.0006		0.0014	0.0004		
Aging	$\alpha$	1.4350	1.7849		1.3182	1.8883		
Adolescent Hump*	$\kappa$		0.0086			0.0097		
Fit (survival curve)^		155.06	12.36		143.07	16.38		
Fit (log of $q_x$ )		3.01	0.74		4.02	0.91		
Fit (death distribution)**		6.21	3.35		18.10	96.16		
Actual Life Expectancy		38.25	38.25		35.93	35.93		
Predicted Life Expectancy		38.43	38.28		36.13	35.94		
Counterfactual Life Expectancy^^			45.86			43.54		

Note: In this table, we fit the model to the 1816 population with and without an exogenous increase in the accident rate occurring in adolescence.

\*The estimate in this row corresponds to the value of the parameter  $\kappa$  after the onset of adolescence. Adolescence starts at age = (-0.0175 x calendar year) + 47.4 for all women, based on the estimates provided in [de La Rochebrochard \(2000\)](#). Adolescence starts one year later for men.

^Our main fit criteria is the sum of squared errors of the survival rate at each age. We also report the fit as the sum of squared errors of the log of  $q_x$  (the probability of dying between ages  $x$  and  $x + 1$ ) and the distribution of deaths. We don't target these moments directly—we target the survival curve.

\*\*To make the fit of the age distribution comparable across columns we use the (normalized) number of deaths as weights.

^^Counterfactual Life Expectancy is computed by holding all estimated parameters fixed and setting the adolescent hump to 0.

Table A2: Robustness checks for 1816

	(1)	(2)	(3)	(4)	(5)	(6)	(7)
	Basic	$\kappa_b$	$\kappa_b$ at $T \sim N()$	$N()$ estimated	Weight	Target death	Truncation at 90
Initial mean health	$\mu_H$	0.8634	0.8917	0.8635	0.7503	0.8020	0.7327
Investment	$I$	0.4075	0.4322	0.4149	0.3712	0.4180	0.4743
Standard Deviation of Shock	$\sigma_e$	1.0241	1.0713	1.0367	0.8369	0.9971	0.9930
Depreciation	$\delta$	0.0006	0.0005	0.0005	0.0005	0.0006	0.0006
Aging	$\alpha$	1.7849	1.8321	1.8153	1.8011	1.7807	1.7950
Adolescent Hump*	$\kappa_a$	0.0086	0.0089	0.0089	0.0112	0.0093	0.0108
Accident rate before adolescence	$\kappa_b$	0.0005					
Mean*			15.6	14.29			
Standard deviation*			1.32	15.71			
Fit (survival curve)^		12.36	13.03	11.49	3.75	15.86	173.74
Fit (log of $q_x$ )		0.74	0.65	0.57	0.40	0.92	1.93
Fit (death distribution)**		3.35	39.55	21.82	2.25	6.89	4.48
Actual Life Expectancy				38.25			
Predicted Life Expectancy		38.28	38.29	38.28	38.26	38.33	39.27
Counterfactual Life expectancy^^		45.86	46.45	46.08	48.82	46.66	49.49

\*Adolescence starts at age = (- 0.0175 x calendar year) + 47.4 in columns 1, 2, 5, 6 and 7. In column 1 we estimate the basic model. In column 2 we allow for the mortality from external causes of death before adolescence to be estimated (we do not set it to 0). In column 3 the timing of adolescence is assumed to follow a normal distribution with mean value (- 0.0175 x calendar year) + 47.4, and standard deviation 1.3285, calculated from the table of 1975 girls in [de La Rochebrochard \(2000\)](#). In column 4 we estimate the mean and the standard deviation of the onset of adolescence. In column 5 we investigate what happens if we use the (normalized) number of deaths as weights in the estimation. In column 6 we use weights and target the distribution of the ages at death instead of the survival curve. In column 7 we use only data up to age 90 to see what the effect of censoring is and because the data after 90 are estimated.

^Our main fit criteria is the sum of squared errors of the survival rate at each age. We also report the fit as the sum of squared errors of the log of  $q_x$  (the probability of dying between ages  $x$  and  $x + 1$ ) and the distribution of deaths. We don't target these moments directly—we target the survival curve.

^^Counterfactual Life Expectancy is computed by holding all estimated parameters fixed and setting the adolescent hump to 0.

\*\*To make the fit of the age distribution comparable across columns we use the (normalized) number of deaths as weights.



Table A3: Estimated parameters for chimpanzees living in the wild

Gender	Model	Female			Male		
		(1)	(2)	(3)	(4)	(5)	(6)
		Basic model	Hump at 8	Hump at 14	Basic model	Hump at 8	Hump at 14
Initial mean health	$\mu_H$	0.9995	1.0337	1.0266	1.8421	3.6402	4.5330
Investment (annual)	$I$	0.3488	0.3613	0.3603	0.7646	1.1364	0.7353
Standard Deviation of Shock	$\sigma_e$	1.1299	1.1806	1.1787	2.7145	4.9725	5.0730
Depreciation	$\delta$	0.0598	0.0600	0.0593	0.0620	0.0510	0.0073
Aging	$\alpha$	0.7627	0.7736	0.7763	1.0319	1.2501	1.8028
Adolescent Hump*	$\kappa$		0.000040	0.000002		0.000378	0.000003
# of individuals at birth		144	144	144	122	122	122
# of moments reported		55	55	55	43	43	43
Fit (survival curve) <sup>b</sup>		111.12	110.20	110.25	128.43	99.26	65.63
Fit (log of $q_x$ )		2.08	2.07	2.09	1.21	1.14	1.06
Actual Life Expectancy		15.38(13.4) <sup>a</sup>	15.38(13.4) <sup>a</sup>	15.38(13.4) <sup>a</sup>	14.47	14.47	14.47
Predicted Life Expectancy		15.35	15.35	15.35	14.52	14.50	14.50

Columns (1) and (4) estimate the model without an adolescent hump. Columns (2) and (4) estimate the model with an exogenous increase in accidents in adolescence at age 8. Columns (3) and (6) estimate the model with an exogenous increase in accidents in adolescence at age 14. Because the data are noisy the second/third model is not a substantially better fit than the first. All are however excellent fits for this population.

Data sources: Life tables for primates in the wild come from [Bronikowski et al. \(2011\)](#). The wild population data come from Brazil, Costa Rica, Kenya, Tanzania, Madagascar and Rwanda.

*a.* Life expectancy in parenthesis corresponds to the one reported in [Bronikowski et al. \(2011\)](#).

*b.* We target the survival curve and compute the sum of squared errors – the data provided are in the form of survival rates.

\*Adolescence starts at age 8.

Table A4: Estimated parameters for French Women and Men for Selected Cohorts

Gender	Females					Males				
	1816	1860	1880	1900	1921	1816	1860	1880	1900	1921
Initial mean health	$\mu_H$	0.9327	0.9034	0.8633	0.9643	1.2051	0.7038	0.7848	0.5812	0.6747
Investment	$I$	0.3724	0.2559	0.2947	0.3296	0.2602	0.4083	0.2455	0.3386	0.4711
Standard Deviation of Shock	$\sigma_e$	0.8296	0.5400	0.5527	0.5215	0.4062	1.0120	0.6200	0.6705	0.8235
Depreciation	$\delta$	0.0005	0.0006	0.0006	0.0006	0.0008	0.0005	0.0006	0.0006	0.0009
Aging	$\alpha$	1.7916	1.6411	1.6248	1.6337	1.4870	1.8048	1.6587	1.6603	1.8540
Adolescent Hump*	$\kappa$	0.0094	0.0077	0.0069	0.0050	0.0022	0.0092	0.0075	0.0079	0.0059
$I$ during WWI/Flu**		0.3722	0.0000	-1.0284	-1.0266			0.1926	-0.6931	-0.0313
$I$ during WWII**			0.2555	0.1035	0.0002	-0.0660		0.0698	0.3101	-0.2086
										0.0021

\*The estimates in this row correspond to the value of the parameter  $\kappa$  after the onset of adolescence. Adolescence starts at age = (-0.0175 x calendar year) + 47.4 for all women, based on the estimates provided in [de La Rochebrochard \(2000\)](#) about the onset of menarche for girls. Adolescence starts one year later for men.

\*\*The estimates in this row correspond to the value of the parameter during the world wars. For example the column for the 1900 female cohort shows that  $I$  was about 0.3296 throughout life but decreased to -1.02 during WWI and to 0.0002 during WWII.

Table A5: Estimated parameters for World Wars for French Men born in 1896

		(1)	(2)
Initial condition	$\mu_H$	1.1417	0.8448
Investment	$I$	0.4548	0.3009
Standard Deviation of Shock	$\sigma_e$	1.0259	0.5983
Depreciation	$\delta$	0.0002	0.0005
Aging	$\alpha$	2.0052	1.6913
Adolescence Hump*	$\kappa$	0.0025	0.0037
WWI Shock**		-1.3104	
Shock in 1914			-2.9302
Shock in 1915			-0.7485
Shock in 1916			-0.5333
Shock in 1917			0.2570
Shock in 1918			-0.1191
WWII Shock**		0.0577	0.1560
Fit (survival curve)^		218.64	11.57
Fit (log of $q_x$ )		2.65	1.27
Fit during WWI (log of $q_x$ )~		1.09	0.09
% Difference in # deaths during WWI~~		-0.14	-0.05
Fit during WWII (log of $q_x$ )~		0.10	0.09
% Difference in # deaths during WWII~~		0.02	-0.11
Actual Life Expectancy		37.94	
Predicted Life Expectancy		37.98	37.96
Counterfactual Life Expectancy without WWI^^		54.13	54.74
Counterfactual Life Expectancy without WWII^^		39.90	39.10
Counterfactual Life eExpectancy^^		56.22	55.97

\*Hump is modeled as a accident rate that starts in adolescence, set to happen at  $(-0.0175 * \text{calendar year}) + 47.4 + 1$  based on the estimates provided in [de La Rochebrochard \(2000\)](#) for the onset of menarche among girls and the assumption that adolescence starts one year later for men.

\*\*The estimates in this row correspond to the value of the parameter during the world wars. For example the first column shows that  $I$  was about 1.1417 throughout life but decreased to -1.3104 during WWI and decreased to 0.0577 during WWII. The same applies to column (2). In column 2, we allow the shocks in investment to vary across years during WWI. The results show that 1914 was the worst year of the war.

^Our main fit criteria is the sum of squared errors of the survival rate at each age. We also report the fit as the sum of squared errors of the log of  $q_x$  (the probability of dying between ages  $x$  and  $x + 1$ ). We don't target these moments directly—we target the survival curve.

^^Counterfactual Life Expectancy is computed by holding all estimated parameters fixed and setting the war parameters to the parameter  $I$ .

~This is computed as sum of squared errors during the war years. A lower number is better.

~~This is computed as  $(\text{predicted} - \text{actual}) / \text{actual}$

To make the fit of the age distribution comparable across columns we use the (normalized) number of deaths as weights.

Table A6: Comparison with alternative mortality models

Cohort	1816					1921				
Model	LMM	G	HP	C	SA	LMM	G	HP	C	SA
<b>Panel A: Women</b>										
<i>Survival curve fit</i>										
RMSE all ages	1.247		0.40	25.78	12.67	1.33		1.08	37.13	6.14
<i>Log of mortality fit</i>										
RMSE (age 45+)	12.05	9.99				3.56	1.34			
RMSE all ages	9.57		9.60	9.61	9.63	3.08		3.08	3.02	3.08
Actual LE	38.28		65.83							
Predicted LE	37.98	-	38.29	17.19	48.09	67.47	-	66.20	69.55	69.37
<b>Panel B Men</b>										
<i>Survival curve fit</i>										
RMSE all ages	1.03		0.49	4.23	5.52	3.28		1.15	2.18	4.90
<i>Log of Mortality fit</i>										
RMSE (age 45+)	14.25	12.10				5.75	3.61			
RMSE all ages	11.44		11.40	11.41	11.40	4.73		4.73	4.73	4.72
Actual LE	35.93		56.14							
Predicted LE	35.94	-	35.95	32.60	39.17	53.65	-	56.65	57.20	58.70
# of parameters	6	2	8	8	6	7	2	8	8	6

note: LMM refers to the model in this paper, G refers to [Gompertz \(1825\)](#), HP refers to [Heligman and Pollard \(1980\)](#), C refers to [Carriere \(1992\)](#) and SA refers to [Sharro and Anderson \(2016\)](#).

## Appendix B: Review of existing models of mortality and contribution of this paper

### Aggregate Models in Demography

The primary objective of demographic modeling efforts has been to develop parsimonious parametric models that provide excellent fits to the data and that therefore can be used in various applications such as pricing annuities or projecting the costs social security. A second important objective has been to characterize the differences in the mortality rates across populations and time periods by comparing the underlying parameters of the model for each population. Here we review canonical models as well and the most recent ones.

In a series of seminal papers starting in 1825, Gompertz observed that mortality rates increased exponentially with age in adulthood, a fact that could be used to price annuities (Gompertz was an actuary). Mathematically, the Gompertz function approximates mortality rates ( $\mu_x$ ) in old ages with a log linear function, with one parameter capturing the intercept ( $\alpha$ ) and the other ( $\beta$ ) capturing the slope of (the log) of mortality with age ( $x$ ):

$$\mu_x = \alpha e^{\beta x}.$$

This model, which came to be known as the Gompertz law, has proved to be an excellent fit for period and cohort data, starting roughly at ages 30-40 and above.<sup>1</sup> The Gompertz law also provides an excellent characterization of the mortality profiles of other species (for a review see [Finch et al. \(1990\)](#)). As a result, subsequent work was devoted to understanding why the Gompertz law arises. The reliability theory from engineer-

---

<sup>1</sup>Previous work has also shown that the slope of mortality with respect to age is remarkably stable across human populations ([Vaupel, 2010](#)) though recent work by [Beltrán-Sánchez et al. \(2012\)](#) shows that the slope of aging varies with early conditions measured by childhood mortality.

ing, which conceptualizes the body as a complex system with many redundant parts, (Gavrilov and Gavrilova, 2001) provided the first mathematical explanation of why the Gompertz law arises.<sup>2</sup> Another important strand of research has investigated the fit of the Gompertz model at very old ages during which mortality appears to plateau instead of continuing its exponential rise.

In a subsequent development Makeham (1860; 1867) noted that some deaths are independent of age, which lead to a modification of the Gompertz law to include a third parameter ( $\gamma$ ), capturing what was described as “extrinsic” or age-independent mortality, in contrast to intrinsic or age-dependent mortality which was captured by the Gompertz law. This extended model is often referred to as the Gompertz-Makeham law:

$$\mu_x = \alpha e^{\beta x} + \gamma.$$

The parsimony and empirical success of the Gompertz model also led to many efforts to develop a “unified” theory of mortality that would characterize the evolution of mortality from birth to death (Carnes et al., 1996). The most successful of these efforts is the model by Heligman and Pollard (1980)—henceforth HP.<sup>3</sup> This is an eight-parameter model that describes the probability of dying ( $q_x$ ) at each age ( $x$ ) and accounts for three distinct phases of mortality: declining mortality in childhood (3 parameters: A, B and C), the adolescent hump (3 parameters: D, E and F) and exponentially increasing mortality in old ages (2 parameters related to the Gompertz curve: G, the intercept at age 0, and H, the slope ).

$$q_x = A^{(x+B)^C} + De^{-E(\ln x - \ln F)^2} + \frac{GH^x}{1 + GH^x}.$$

---

<sup>2</sup>More recent efforts have tested and refined these theories. See Mitnitski et al. (2015) for a summary. There are several alternative models of aging, for example another set of theories argues that aging is the result of genetic regulated processes (e.g. Moody and Sasser, 2020). A key issue is whether health deteriorates as a function of deficits/failures or as a function of the passage of time (or both).

<sup>3</sup>Siler (1979, 1983) provided a six parameter model from birth to death. However, this model does not fit many populations well as it fails to account for the adolescent accident hump.

A large number of subsequent papers has used this model and demonstrated that it provides an excellent fit for period data from various contexts as [Sharrow et al. \(2013\)](#) describe. This model is popular for several reasons: it is parsimonious, it fits the data well and the parameters have natural interpretations that make it a useful tool in comparing populations.

Other models have been developed since. For example [Carriere \(1992\)](#) introduces a parametric model with slightly better fit for the US male and female 1980 CSO tables. The survival function in [Carriere \(1992\)](#) is a mixture of a Weibull, Inverse-Weibull, and a Gompertz function, and is determined by 8 parameters:

$$s(x) = \psi_1 \exp \left\{ - \left( \frac{x}{m_1} \right)^{\frac{m_1}{\sigma_1}} \right\} + \psi_2 \left[ 1 - \exp \left\{ - \left( \frac{x}{m_2} \right)^{\frac{m_2}{\sigma_2}} \right\} \right] + (1 - \psi_1 - \psi_2) \exp \left\{ e^{-\frac{m_3}{\sigma_3}} - e^{-\frac{x-m_3}{\sigma_3}} \right\}$$

Although the HP model provides an excellent fit to the data it does not break down mortality into different types or causes. A recent paper by [Sharrow and Anderson \(2016\)](#) provides an alternative model that separate mortality into extrinsic and intrinsic lifespans (building on earlier work by [Li and Anderson \(2013\)](#), and extending the Gompertz-Makeham law to all ages). Roughly speaking, extrinsic factors correspond to changes in infectious disease and other factors that the environment imposes on the individual; and intrinsic factors are changes in way the body functions and roughly correspond to changes in chronic (non-communicable) diseases. The model has two functions that characterize extrinsic mortality in childhood and mid-life, and one that characterizes intrinsic mortality in old age. This model does characterize the evolution of mortality from birth to death, but the authors fit their model to period not cohort data. Their objective is to separate into causes of decline, not to provide a model that is a better fit to the data than previous ones, or to explain other phenomena.

The HP model is also not well suited to understand how insults early in life affect mortality later in life. [Palloni and Beltrán-Sánchez \(2017\)](#) have a model of Barker frailty,

linking frailty early in life with mortality at various points in the lifetime. It characterizes frailty in three portions of the lifetime, where frailty results in excess mortality early and late in life but not in the middle portion. This paper does not estimate the model, it conducts simulations to understand the effects of increasing frailty on mortality patterns. This model is not estimated with any data so it is difficult to assess how it would compare to other models in terms of fit, including ours.

All demographic models describe aggregate mortality rates as a function of various parameters.

This paper makes main contributions to the existing literature in demography. First, we provide a parsimonious and tractable production function that describes the evolution of a population's health and mortality starting at birth that is suited for tracking the long-term impacts of various insults and investments. To that end, our approach differs in one fundamental aspect from the demographic approach just described. As in the seminal [Grossman \(1972\)](#) model, we model directly how the health stock of each individual evolves, rather than only modeling the mortality or survival rates of the aggregate population.

Like the HP model, our model is flexible enough to provide an excellent fit for the mortality profiles of more than 100 cohorts we study. But our approach is better suited for studying how various shocks affect the health and mortality of the population overtime — we can easily model inputs into health directly and trace their effects as cohorts age by tracking the evolution of the distribution of health. Relative to the recent models our model has some advantages. Like [Sharroff and Anderson \(2016\)](#) we decompose mortality into two separate causes of death, extrinsic and intrinsic. Like [Palloni and Beltrán-Sánchez \(2017\)](#) we can use our model to study Barker frailty. Our model accomplishes both aims within the same framework.

The second main contribution of this paper is to show that simple modifications of this baseline model explain a wide range of existing demographic phenomena. We demon-



strate this by studying the effects of increasing lifetime resources, and the impact of negative in utero shocks on a population's subsequent average health and mortality. We also study the effects of temporary shocks such as wars or bad weather. To our knowledge there is no other model that both provides an excellent fit to the cohort data and that can also explain the variety of phenomena we study.

Before moving onto the economics models, we also note that our paper builds on the classic demographic work by [Vaupel et al. \(1979\)](#) to introduce heterogeneity in the population from birth onwards.

## Models of Individual Mortality in Economics

Economic models of health and mortality were not developed with the aim of fitting aggregate demographic data. Instead, they were developed to understand health expenditures and health behaviors and thus focus on how individuals would maximize their wellbeing (or utility) which depends on health and consumption. In addition to including parameters that govern the evolution of health and longevity, these models also include other “deep” parameters regulating for example the extent to which individuals value health relative to consumption or their discount rates.

The study of health and health behaviors in economics dates back to the seminal model of [Grossman \(1972\)](#). The objective of this model is to derive the demand for medical care (and thus to explain medical care spending) as a function of an individual's characteristics (including education and other traits), their wages and the prices of medical care. The model posits that the demand for medical care is derived from the demand for health, which individuals value itself (it has consumption value) and because health affects productivity in the labor market and thus affects wages. Because health is the ultimate good individuals are after, Grossman models its evolution until an individual dies. Importantly, Grossman's model assumes i) that individuals face a constantly depreciating health, which depreciates as a function of the existing stock, and ii) that they can invest

in (and restore) their health by purchasing market goods and services and investing their own time. In this model factors that affect the cost of these investments (such as wages or prices) modify behavior and ultimately health and mortality.

This model is the starting point for almost all studies in economics that investigate individual health and mortality. Its insights have been cited to explain a wide range of phenomena, including, for example, SES gradients in health. There have also been several attempts to estimate this model using cross sectional and more recently panel data (for a review of early attempts, see [Grossman \(2004\)](#)). However, these attempts have rejected the Grossman model empirically on a number of dimensions. For instance the model predicts that health investments are highest for the healthiest individuals, whereas the data show the opposite is true (for a recent summary of these attempts, see [Hartwig and Sturm \(2018\)](#)).

Over the years the model has faced further criticism. Particularly relevant to our contribution, previous authors have noted that the model is unrealistic in its conception of health. In [Grossman \(1972\)](#)'s model individuals can perfectly restore their health and in principle they could live forever. The model also starts with adults. Thus, a number of models have been developed to address some of these issues. Two recent models address some of the limitations of the Grossman model.

[Galama and Van Kippersluis \(2019\)](#)'s model is designed to understand how socio-economic status affects health over the life cycle. The original Grossman model allows for differences in education and income/wages to affect the demand for health through limited channels. However empirical work has demonstrated that the SES gradient in health likely operates through many other dimensions (e.g., job related stress, affecting the rate of health deterioration), which Galama and van Kippersluis incorporate. Galama and van Kippersluis calibrate their model and show that its predictions are consistent with observations in the literature.

[Dalgaard and Strulik \(2014\)](#) develop an alternative model where individuals also make

multiple choices regarding consumption, savings and health investments. They use this model to assess if the famous Preston curve, relating GDP to life expectancy, can be understood as resulting from the effects of income on longevity through investments. The key difference in this model is how aging is modeled: based on insights from gerontology, aging is described as the result of cumulative health deficits. The authors calibrate the model and then show that changes in GDP generate predictions that line up with the observed Preston curve. Unlike the Grossman model, this model predicts that unhealthy individuals spend more on health than healthy individuals, and they cannot live forever regardless of how much they invest in health.

Like all the previous economic models, both [Galama and Van Kippersluis \(2019\)](#)'s and [Dalgaard and Strulik \(2014\)](#)'s models start in adulthood. [Dalgaard et al. \(2019\)](#) extend the previously developed health deficit model of [Dalgaard and Strulik \(2014\)](#) to incorporate the childhood period to be able to study the long-term impact of in utero and childhood conditions. During the childhood period individuals grow. They calibrate this model and show that in contrast to the Grossman model, this model predicts that differences in health early in life are amplified during the lifetime of individuals. They do not make predictions about mortality profiles.

Our basic model is more parsimonious than the original Grossman model, or its most recent successors in the economics literature ([Dalgaard and Strulik \(2014\)](#) or [Galama and Van Kippersluis \(2019\)](#)). These models were developed to understand health expenditures and health behaviors and thus focus on how individuals would maximize their wellbeing (or utility) which depends on health and consumption. As a result, these economic models can only be estimated if one has access to incomes/wages, prices, health care utilization and other variables. We use data on mortality alone to calibrate our model. We focus on a production process only and ignore maximizing behavior, at least initially. In this dimension, our model differs in a number of other dimensions from the original Grossman model. For example, we do not impose a maximum life expectancy, we incor-

porate stochastic shocks, we allow for differences in initial endowments and our aging process does not depend on the level of health.

Our main innovation relative to these more ambitious models is to provide a unified framework for health and mortality at all ages, including childhood. Including this key childhood period allows us to match the pattern of declining mortality among children (up to adolescence). Alternative state-of-the art models, such as [Dalgaard and Strulik \(2014\)](#)’s accumulating health deficits model, or [Galama and Van Kippersluis \(2019\)](#)’s theory of socioeconomic status and mortality, start with adults and thus cannot account for this feature of the data.

[Dalgaard et al. \(2019\)](#) extend [Dalgaard and Strulik \(2014\)](#)’s model to include a childhood period, but they do so by adding a separate health production function for childhood. Instead, our framework is able to describe aging from birth to old ages with the same law of motion, where mortality declines during childhood due to both selection effects and investments. We also demonstrate that the model fits mortality curves for entire cohorts well, which more ambitious economic models have not demonstrated. To our knowledge, there is no other model that has accurately (empirically) predicted the lifetime health and mortality of populations, while providing a law of motion for health at the individual level. By tracking the evolution of health for all individuals in entire population and its mortality consequences, our model provides a framework that bridges the economic and demographic approaches and upon which more complex models that incorporate behaviors can be built and estimated.

It is worth noting that our model’s predictions for the effects of in utero shocks do not perfectly align with those of the health deficit model as we note in the text: [Dalgaard et al. \(2019\)](#)’s model of health deficits also predicts that in-utero shocks will result in health gaps that increase with age starting in adulthood. Our model predicts a U-shape pattern of effects rather than a monotonically increasing effect. This U-shape results from our having an early childhood period where investments move the distribution of health up.

## Appendix C: Mathematical appendix

The model is defined as follows:

$$\begin{cases} H_a = H_{a-1} - d(a) + I + \varepsilon_t & \text{if } D_{a-1} = 0 \\ D_a = \mathbb{I}(H_a \leq \underline{H}, D_{a-1} = 0), \\ D_0 = 0 \end{cases} \quad (1)$$

with  $d(a) = \delta \cdot a^\alpha$   $\delta \in (0, \infty)$ ,  $\alpha \in (0, \infty)$ , and  $I \in \mathbb{R}$ .  $\underline{H}$  and  $\sigma_H^2$  are normalized to be 0 and 1, respectively. Let  $\hat{H}_a \equiv \mathbb{E}[H_a \mid H_a > 0]$  denote the average health in the living population with age  $a$  and  $\sigma_{\hat{H}_a} \equiv \text{Var}[H_a \mid H_a > 0]$  the variance of health among the living.

**Proposition 1.** *Everyone dies eventually.*

The cumulative distribution function of our process can be bounded above by a process easier to study. Consider the process  $\{H_a^*\}_{a=1}^\infty$ , defined by  $H_0^* = H_0 \sim \mathcal{N}(\mu_H, \sigma_H^2)$  and the recurrence relation:

$$H_a^* = H_{a-1}^* + I - \delta \cdot a^\alpha + \varepsilon_a, \quad \varepsilon_a \sim \mathcal{N}(0, \sigma_\varepsilon^2) \quad (2)$$

The process is similar to the one in our model except that there is no truncation. It is easy to tell that  $0 \leq P(H_a > z) \leq P(H_a^* > z)$  for any  $z > 0$ . Now for any  $a \geq 0$ ,  $H_t^*$  is normally distributed with mean

$$\mu_{H_a^*} = \mu_H + I \cdot a - \delta \sum_{k=1}^a k^\alpha \quad (3)$$

and standard deviation

$$\sigma_{H_a^*} = \sqrt{\sigma_H^2 + a \cdot \sigma_\varepsilon^2} \quad (4)$$

Hence,  $P(H_a^* > z) = 1 - \Phi\left(\frac{z - \mu_{H_a^*}}{\sigma_{H_a^*}}\right)$ , where  $\Phi$  is the CDF of the standard normal distribution. As  $a \rightarrow \infty$ , we have  $\mu_{H_a^*} \sim I \cdot a - \delta \cdot \frac{a^{\alpha+1}}{\alpha+1}$  and  $\sigma_{H_a^*} \sim \sqrt{a} \cdot \sigma_\varepsilon$ . Therefore if  $\alpha > 0$ ,  $\frac{\mu_{H_a^*}}{\sigma_{H_a^*}} \rightarrow -\infty$  as  $a \rightarrow \infty$ .

**Remark: Extended model with Accident shocks** Proposition 1, 2 and 3 hold for the extended model with accident shocks drawn independently from the health status. Because accident shocks are drawn independently from the health status, they leave the *cdf* of health unchanged and therefore the proofs are unaffected.

## Appendix D: Notes on the empirical methods

### 1. Data

**Territory changes.** The table below describes the details of the changes in territory that took place in France since 1816.

Year	Territorial Changes
1861	Annexation of Savoie and Haute-Savoie, and of <i>Comte de Nice</i>
1869	Franco-Prussian war: loss of Alsace-Lorraine
1914	WWI: East of France, is occupied by German military.
1919	At the end of WWI, Alsace-Lorraine is re-integrated to French territory
1939	WW2: Loss of Alsace-Lorraine
1943	WW2: Loss of Corsica
1945	Current territory: Alsace-Lorraine and Corsica re-integrated to French territory

These changes in territory results in large changes in the population and death counts.

This is illustrated below for population. It is unclear how to compute mortality in the year of the change. We compute it by using a weighted average of the population at the beginning and end of the year.

**Migration.** In the HMD, cohort population counts are available. However, because of migrations, these counts cannot be used to derive a survival curve for a cohort. Because of net positive immigration occurring in France, the number of individuals in a given cohort can even increase from one year to the next. This is especially true at the end of the Algerian Independence War. (e.g. the size of the female cohort born in 1910 increases from 300,369 to 303,273 between 1962 and 1963, despite a reported mortality rate of 0.5162. The unit of analysis in our model of mortality is a country cohort, hence abstracts from migration. In our model the mortality rates coincide exactly with the slope of the survival curve. This is not true in the HMD. The population of the cohort melts natives and immigrants of the same age.

## 2. Computing the death rates, survival rates and life expectancy

**Death rates.** When taking our model to the data we target the most direct counterpart of our modeled cohort “mortality rate”, which is computed as the number of individuals who died during a year, divided by the number of individuals alive at the beginning of the day. Technically, we compute annual probabilities of dying at a given age instead of rates. We make no adjustments for the fact that the deaths in the first year do not correspond to individuals born that year.

In typical life tables this number corresponds to what demographers call  $q_t$ , the probability of dying in a given year, and is conceptually distinct to the mortality rate, denoted by  $m_t$ . The main difference lies in adjusting the denominator — the size of the population. As more individuals die during the year the population needs to be adjusted to estimate the size of the remaining population exposed to the risk of death. Because our baseline model does not take this adjustment into account, we compute a direct counterpart of our theoretical object. Therefore, we compute the raw death rate in year  $t$  for a given cohort,  $q_t$ , as follows:

$$q_t = \frac{D_t}{N_t}$$

where  $D_t$  is the death count for year  $t$  from the HMD cohort table and  $N_t$  is the population on January 1st of year  $t$ . The HMD makes adjustments to compute a probability that is corrected for the fact that the data do not track the same individuals over time, so the probability of dying is not correctly computed for a given cohort. The  $q$  we estimate with the raw counts is very similar to what is reported by the HMD except for the first year of life and the last years of life as shown in Appendix Figure A9. This results in our underestimating life expectancy somewhat.

**Survival curves.** We compute the survival curve recursively as follows. After initial-



izing  $S_0 = 100$ , we iteratively compute:

$$S_t = S_{t-1} \times (1 - q_{t-1})$$

**Life expectancy.** Life Expectancy (LE) is an important statistics for the health profile of a given cohort. We compute LE as a way of comparing our model to the data in a parsimonious way. While we try to provide informative estimates of cohort life expectancy, we do not claim that their accuracy is comparable to demographic studies. Nevertheless, as we treat the series generated by our model in exactly the same manner as the data series, we obtain pairs of LE that are readily comparable.

### 3. Estimation routine

We compute our estimates using Matlab's canned *fminsearch* routine, a downhill simplex method, and Powell (1964)'s conjugate direction method. We first estimate the model using *fminsearch* until the objective function changes by less than  $10^{-3}$ . The objective function is the sum of squared errors between the model's survival's curve and the one from the data. We then use these estimates as starting values for Powell's routine. Once Powell's routine converges, we use the estimated values from this procedure and implement *fminsearch* again until it converges. The total estimations on the UCLA computing cluster takes several hours. We experimented with different initial values for the parameters. The reported estimates correspond to the lowest final function value.

### 4. Bootstrapping standard errors

Estimates from sample data come with standard errors. However, the mortality rates in the HMD are computed from birth certificates of the total population, not a sample of it. A typical cohort in our study counts 400,000 individuals. As a result, the standard errors are negligible and all of the parameter uncertainty comes from model misspecification

and data inaccuracy rather than sampling variation. We therefore do not report standard errors for the French cohorts.

In contrast, we do compute the standard errors for the chimpanzee estimates as the data in that case consist of samples of one or two hundreds of individuals. One way of bootstrapping the standard errors, given a series of mortality rates for a cohort, is to view each sample of size  $N$  as a sequence of Bernoulli trials with varying success rates. Alternatively, one can view the survival curve of a population of size  $N$  as an  $N \times 1$  vector of age at death. One can produce bootstrap estimates by drawing with replacement  $M$  subsamples of size  $N$  and compute the empirical survival curve.

## 5. Estimation of Wars/pandemics in time series

We estimate the complete times series for females only. We model WWI and WWII as lowering the level of  $I$  during the event, which is set to start in 1918 and last one year in the case of the flu pandemic for women—this choice is motivated by the data which shows that WWI did not result in an increase in mortality for them, but instead mortality increased dramatically as a result of the Flu (see Appendix Figure A10). For men we lower  $I$  from 1914 to 1919 (see Appendix Table 5). For WWII we lower  $I$  from 1939 to 1945.

## 6. Estimation of alternative mortality models

We estimate four alternative models of mortality. We use the R package “MortalityLaws” version 1.9.3 (developed by [Pascariu and Canudas-Romo, 2022](#)) to estimate the [Gompertz \(1871\)](#), [Heligman and Pollard \(1980\)](#) and [Carriere \(1992\)](#) models, and the package “vitality” version 1.3 (developed by [Passolt et al., 2018](#)) to estimate the [Sharro and Anderson \(2016\)](#) model.<sup>4</sup> We estimate the Gompertz model for age 45 onwards only. All models are

<sup>4</sup>While usually estimated on period data for practical reasons, several of these models have a natural “cohort” interpretation, e.g. the vitality process in [Sharro and Anderson \(2016\)](#) alludes to physiological processes occurring at the individual level.

estimated only up to age 100. We use the predicted values from each model to compute

the RMSE, as  $RMSE = \sqrt{\frac{1}{100} \sum_{a=0}^{99} (y_a - \hat{y}_a)^2}$

## Appendix E: Implications for optimal investments

### Optimization in a stationary environment

So far we have considered a population that receives constant investments in its health, uniformly over the lifetime. But is that behavior a reasonable approximation if resources are optimally allocated over the lifetime? To answer this question, this section relaxes the simplifying assumption of constant investment, and estimates the optimal investment profile that a social planner concerned with maximizing the life-expectancy of a population would choose. Remarkably, while this optimal investment profile indeed deviates from the constant investment rule studied in the previous sections, it would result in very similar patterns of mortality. In other words, the optimal investment sequence does not fundamentally change the age-profile of mortality rates. We then evaluate the life expectancy gains resulting from optimization.

First, we develop notation to describe the problem that a benevolent social planner would face. We solve this problem under two key assumptions. The first key assumption is that the planner has a fixed budget but has the ability to borrow and save costlessly — in other words, the planner knows exactly what the total lifetime resources are for a given cohort and can redistribute these resources across the lifetime at no cost.<sup>5</sup> The second assumption we make is that the planner wishes to maximize life expectancy.

The survival function tracks the probability of surviving over time. It is naturally expressed as a function of the cdf of health in the population. The probability of surviving until the end of period  $a$  is  $S_a = 1 - F_a(0)$ . Life expectancy at birth for a given cohort is conveniently related to the survival function

$$LE = \sum_{a=1}^{\infty} S_a$$

---

<sup>5</sup>This is a standard set of assumptions in this type of models, for example see [Murphy and Topel \(2006\)](#).

Several observations are in order. First, in practice, this is a finite sum. Second, this is the cohort's life expectancy, not the "period" life expectancy which is usually reported. The social planner now chooses an investment path  $\mathcal{I} = \{I_a\}_{a \in \mathbb{N}}$  that is age-dependent, instead of keeping the investment level  $I$  constant over the lifetime. The planner can move resources over time periods costlessly, as if a perfect annuity were available, and faces a given lifetime budget,  $B$ . Then the optimization problem takes the form

$$\begin{aligned} \max_{\mathcal{I}} LE(\mathcal{I}) &= \max_{\{I_a\}} \sum_{a=1}^{\infty} S_a(\mathcal{I}) \\ s.t. \quad &\sum_{a=1}^{\infty} I_a \cdot S_a(\mathcal{I}) \leq B \end{aligned}$$

The social planner chooses an optimal path such that the marginal effect of increasing investment at a given age is equalized across all ages. The first order conditions are given by

$$\sum_{s=a}^{\infty} \frac{\partial S_s(\mathcal{I})}{\partial I_a} - \lambda \left[ S_a(\mathcal{I}) + \sum_{s \geq a} I_s \frac{\partial S_s(\mathcal{I})}{\partial I_a} \right] = 0, \forall a > 0$$

where  $\lambda$  is the Lagrange multiplier and therefore  $\frac{1}{\lambda}$  represents the shadow cost for the social planner, starting from the optimal path, of an additional year of life expectancy. Both terms in the bracket are positive, illustrating the key dynamic tradeoff in investment with a fixed budget. An additional investment at one age increases the number of survivors at all subsequent ages, exerting greater pressure on the budget at all subsequent periods. Intuitively, this channel gets weaker and weaker at older ages because mortality rates are high at old ages even with investments. While we were unable to formally make this point analytically, we show numerically that this intuition is valid in the range of parameters estimated from the data.

## Timing of optimal investments, polynomials

To estimate the optimal investment, we follow a lower-dimensional sieves estimation method.<sup>6</sup> We start by approximating the investment profile over age with a first order function of age (adding 2 parameters) and then with a second order polynomial (3 more parameters). We impose the constraint that the total spending per cohort is the same as the budget resulting from our estimated constant lifetime investment i.e.  $B = \sum_{a=1}^{100} \hat{I} \cdot S_a(\mathcal{I})$ . Given budget  $B$  we run a grid search to find the quadratic investment profile that maximizes the life expectancy of the cohort.

The results of this exercise are displayed in Appendix Figure A21. Relative to the case with a constant function, an optimal linear investment function redistributes more resources to the young. If we allow a quadratic term then we find that a U-shape investment profile is optimal to maximize the average life-expectancy in the population (panel a). Our original model sets  $I$  to be constant in levels. But in percentage terms, relative to the baseline level of health at a given age,  $I$  was already U-shaped in the basic model. What we find then is that the optimal investment is even more U-shaped — it transfers additional resources to the young and the old, away from the middle-aged individuals.

These results show that optimal health investments are largest when health is at its lowest — that is, at very young and very old ages. Interestingly, health care expenditures by age in most countries actually follow this age-profile ([Alemayehu and Warner, 2004](#)). These findings are also consistent with empirical findings which show that health and the demand for medical services are negatively correlated ([Wagstaff, 1986](#)) and that medical expenditures rise sharply with age (e.g. [De Nardi et al. 2010](#)).<sup>7</sup>

---

<sup>6</sup>A fully nonparametric approach for the optimal investment profile over the lifetime would require optimizing over a hundred or so parameters (one for each age) for each cohort. In the absence of a closed-form solution, this is impractical. It is also not feasible since we have 100 data points: if we allow for a unique investment level at every age we are under-identified (we would have 100 data points and at least 106 parameters to estimate).

<sup>7</sup>These results are in contrast with the predictions of the Grossman model which predicts that investments would decline with age as individuals near death. See [Wagstaff \(1986\)](#) for an early discussion, or [Strulik \(2015\)](#) for a more recent discussion of this issue.

Panel b shows the mortality curves before and after optimization — they have the same basic shape we have observed. The resulting survival curves are flatter in adulthood and steeper in old ages, suggesting the rectangularization of survival might be in part associated with the emergence of optimal investments. Optimizing investment results in a gain of about 3 years of life expectancy in the specific case we show in Appendix Figure A21, based on the estimated parameters for French women born in 1816.

**Optimization when budgets depend on health.** We have solved the optimization problem under the assumption that stock of available resources is not influenced by the health of the population. But if food and other resources are produced rather than taken from the environment, health is likely to impact resources by affecting the work capacity of the population. Indeed, nutrition levels and disease rates have been shown to affect productivity and wages (Thomas et al., 2004). They also affect inputs into wages such as cognition and education (Field et al., 2009). Many empirical studies report a correlation between income and health (Cutler et al., 2012, Chetty et al., 2016) as noted above. While our baseline model embeds the effect of resources on health, a causal link going in the other direction is also likely at play: people who get sick or are hospitalized suffer a subsequent drop in income (Smith, 1999, Dobkin et al., 2018). With panel data on wages, it would be possible to improve on our estimates to account for these effects.

**Overlapping generations.** Another natural extension would be to embed our model in an overlapping generations setting to reflect the fact that most social insurance programs, including health care insurance, involve transfers across cohorts at a given point in time, rather than within-cohort transfers over time (as we have considered here for simplicity). An overlapping generation model could also be used to link the health of the parents with that of their children, a mechanism that has found some support in the empirical literature.

## References

- Alemayehu, Berhanu and Kenneth E. Warner**, "The lifetime distribution of health care costs," *Health services research*, 2004, 39 (3), 627–642.
- Almond, Douglas and Janet Currie**, "Killing me softly: The fetal origins hypothesis," *The Journal of Economic Perspectives*, 2011, 25 (3), 153–172.
- Beltrán-Sánchez, Hiram, Eileen M Crimmins, and Caleb E Finch**, "Early cohort mortality predicts the rate of aging in the cohort: A historical analysis," *Journal of developmental origins of health and disease*, 2012, 3 (5), 380–386.
- Bronikowski, Anne M., Jeanne Altmann, Diane K. Brockman, Marina Cords, Linda M. Fedigan, Anne Pusey, Tara Stoinski, William F. Morris, Karen B. Strier, and Susan C. Alberts**, "Aging in the natural world: comparative data reveal similar mortality patterns across primates," *Science*, 2011, 331 (6022), 1325–1328.
- Carnes, Bruce A., S. Jay Olshansky, and Douglas Grahn**, "Continuing the search for a law of mortality," *Population and Development review*, 1996, pp. 231–264.
- Carriere, Jacques F.**, "Parametric models for life tables," *Transactions of the Society of Actuaries*, 1992, 44, 77–99.
- Chetty, Raj, Michael Stepner, Sarah Abraham, Shelby Lin, Benjamin Scuderi, Nicholas Turner, Augustin Bergeron, and David Cutler**, "The association between income and life expectancy in the United States, 2001-2014," *Jama*, 2016, 315 (16), 1750–1766.
- Cutler, David M., Adriana Lleras-Muney, Tom Vogl, S. Glied, and P. C. Smith**, "Socioeconomic Status and Health: Dimensions and Mechanisms," in "The Oxford Handbook of Health Economics," Oxford University Press, 2012.
- Dalgaard, Carl-Johan and Holger Strulik**, "Optimal aging and death: understanding the Preston curve," *Journal of the European Economic Association*, 2014, 12 (3), 672–701.



- , Casper Worm Hansen, and Holger Strulik, “Accounting for fetal origins: Health capital vs. health deficits,” *Health Deficits* (October 19, 2019), 2019.
- de La Rochebrochard, Elise**, “Age at puberty of girls and boys in France: Measurements from a survey on adolescent sexuality,” *Population: An English Selection*, 2000, pp. 51–79.
- Dobkin, Carlos, Amy Finkelstein, Raymond Kluender, and Matthew J Notowidigdo**, “The economic consequences of hospital admissions,” *American Economic Review*, 2018, 108 (2), 308–52.
- Field, Erica, Omar Robles, and Maximo Torero**, “Iodine deficiency and schooling attainment in Tanzania,” *American Economic Journal: Applied Economics*, 2009, 1 (4), 140–169.
- Finch, Caleb E, Malcolm C Pike, and Matthew Witten**, “Slow mortality rate accelerations during aging in some animals approximate that of humans,” *Science*, 1990, 249 (4971), 902–905.
- Galama, Titus J and Hans Van Kippersluis**, “A theory of socio-economic disparities in health over the life cycle,” *The Economic Journal*, 2019, 129 (617), 338–374.
- Gavrilov, Leonid A and Natalia S Gavrilova**, “The reliability theory of aging and longevity,” *Journal of theoretical Biology*, 2001, 213 (4), 527–545.
- Gompertz, Benjamin**, “On the nature of the function expressive of the law of human mortality, and on a new mode of determining the value of life contingencies,” *Philosophical transactions of the Royal Society of London*, 1825, 115, 513–583.
- , “On one uniform law of mortality from birth to extreme old age, and on the law of sickness,” *Journal of the Institute of Actuaries and Assurance Magazine*, 1871, 16 (5), 329–344.
- Grossman, Michael**, “On the concept of health capital and the demand for health,” *Journal of Political economy*, 1972, 80 (2), 223–255.

—, “The demand for health, 30 years later: a very personal retrospective and prospective reflection,” *Journal of health economics*, 2004, 23 (4), 629–636.

**Hartwig, Jochen and Jan-Egbert Sturm**, “Testing the Grossman model of medical spending determinants with macroeconomic panel data,” *The European Journal of Health Economics*, 2018, 19 (8), 1067–1086.

**Heligman, Larry and John H. Pollard**, “The age pattern of mortality,” *Journal of the Institute of Actuaries*, 1980, 107 (01), 49–80.

**Human Mortality Database**. University of California, Berkeley (USA), and Max Planck Institute for Demographic Research (Germany). Available at [www.mortality.org](http://www.mortality.org). Data downloaded in August 2017.

**Li, Ting and James Anderson**, “Shaping human mortality patterns through intrinsic and extrinsic vitality processes,” *Demographic research*, 2013, 28, 341–372.

**Makeham, William Matthew**, “On the law of mortality and the construction of annuity tables,” *Journal of the Institute of Actuaries*, 1860, 8 (6), 301–310.

—, “On the law of mortality,” *Journal of the Institute of Actuaries*, 1867, 13 (6), 325–358.

**Mitnitski, Arnold, Joanna Collerton, Carmen Martin-Ruiz, Carol Jagger, Thomas von Zglinicki, Kenneth Rockwood, and Thomas BL Kirkwood**, “Age-related frailty and its association with biological markers of ageing,” *BMC medicine*, 2015, 13 (1), 1–9.

**Moody, Harry R and Jennifer R Sasser**, *Aging: Concepts and controversies*, Sage publications, 2020.

**Murphy, Kevin M. and Robert H. Topel**, “The value of health and longevity,” *Journal of political Economy*, 2006, 114 (5), 871–904.

**Nardi, Mariacristina De, Eric French, and John B Jones**, “Why do the elderly save? The role of medical expenses,” *Journal of political economy*, 2010, 118 (1), 39–75.

- Palloni, Alberto and Hiram Beltrán-Sánchez**, “Discrete Barker Frailty and warped mortality dynamics at older ages,” *Demography*, 2017, 54 (2), 655–671.
- Pascariu, Marius D and Vladimir Canudas-Romo**, “Package "MortalityLaws",” 2022.
- Passolt, Gregor, James J Anderson, Ting Li, David H Salinger, David J Sharrow, and Maintainer David J Sharrow**, “Package "Vitality",” 2018.
- Schwandt, Hannes and Till M Von Wachter**, “Socioeconomic decline and death: Midlife impacts of graduating in a recession,” Technical Report, National Bureau of Economic Research 2020.
- Sharrow, David J. and James J. Anderson**, “Quantifying Intrinsic and Extrinsic Contributions to Human Longevity: Application of a Two-Process Vitality Model to the Human Mortality Database,” *Demography*, 2016, 53 (6), 2105–2119.
- Sharrow, David J, Samuel J Clark, Mark A Collinson, Kathleen Kahn, and Stephen M Tollman**, “The age pattern of increases in mortality affected by HIV: Bayesian fit of the Heligman-Pollard model to data from the Agincourt HDSS field site in rural northeast South Africa,” *Demographic research*, 2013, 29, 1039.
- Siler, William**, “A competing-risk model for animal mortality,” *Ecology*, 1979, 60 (4), 750–757.
- , “Parameters of mortality in human populations with widely varying life spans,” *Statistics in medicine*, 1983, 2 (3), 373–380.
- Smith, James P.**, “Healthy bodies and thick wallets: the dual relation between health and economic status,” *The journal of economic perspectives: a journal of the American Economic Association*, 1999, 13 (2), 144.
- Strulik, Holger**, “A Closed-form Solution for the Health Capital Model,” *Journal of Demographic Economics*, 2015, 81 (3), 301–316.

**Thomas, Duncan, Elizabeth Frankenberg, Jed Friedman, Jean-Pierre Habicht, Nathan Jones, Christopher McKelvey, Gretel Peltz, Bondan Sikoki, James P. Smith, Cecep Sumantri, and others,** "Causal effect of health on labor market outcomes: Evidence from a random assignment iron supplementation intervention," *California Center for Population Research*, 2004.

**Toulemon, Laurent and Magali Barbieri,** "The mortality impact of the August 2003 heat wave in France: investigating the 'harvesting' effect and other long-term consequences," *Population studies*, 2008, 62 (1), 39–53.

**Vaupel, James W,** "Biodemography of human ageing," *Nature*, 2010, 464 (7288), 536–542.

**Vaupel, James W., Kenneth G. Manton, and Eric Stallard,** "The impact of heterogeneity in individual frailty on the dynamics of mortality," *Demography*, 1979, 16 (3), 439–454.

**Wagstaff, Adam,** "The demand for health: some new empirical evidence," *Journal of Health economics*, 1986, 5 (3), 195–233.